Macromolecules

ARTICLE

pubs.acs.org/Macromolecules

Rubber−Filler Interactions and Network Structure in Relation to Stress−Strain Behavior of Vulcanized, Carbon Black Filled EPDM

V. M. Litvinov,[†,‡,*] R. A. Orza,[‡,§] M. Klüppel,[⊥] M. van Duin,[∥] and P. C. M. M. Magusin[§]

[†]DSM Resolve, P.O. Box 18, 6160 MD Geleen, The Netherlands

[‡]Dutch Polymer Institute, P.O. Box 902, 5600 AX Eindhoven, The Netherlands

[§]Eindhoven University of Technology, P.O. Box 513, 5600 MB Eindhoven, The Netherlands

[⊥]Deutsches Institut für Kautschuktechnologie e.V., Eupener Strasse 33, D-30519 Hannover, Germany

[∥]Lanxess Elastomers Global, R&D, P.O. Box 1130, 6160 BC Geleen, The Netherlands

ABSTRACT: Immobilization of EPDM chains on the surface of carbon black and network structure in the rubber matrix of filled EPDM rubbers were studied by low-field proton NMR experiments. Advanced NMR experiments unambiguously show strong immobilization of EPDM chain fragments on the surface of carbon black. The thickness of the immobilized EPDM−carbon black interfacial layer is estimated to be ≥0.6 nm. The average number of monomer units per adsorption site is approximately nine, which suggests preferential chain adsorption at the crystal boundaries of carbon-black particles. The adsorbed chain fragments form physical (adsorption) junctions restricting chain mobility in the rubbery matrix outside of the interface. The cross-link density in filled EPDM is determined as a function of the filler type and its amount. The contribution of adsorption junctions to the total cross-link density is moderate as compared to the density of chemical cross-links and entanglement density. The mechanically effective network density in carbon-black-filled vulcanizates is determined by analysis of the stress−strain curves on the basis of the dynamic flocculation model. Comparison of the network density as measured by NMR and mechanical experiments shows significant differences which helps in better understanding of the reinforcement mechanism of filled rubbers. The study demonstrates that a relatively small amount of strongly adsorbed chains impacts the stress−strain properties of filled elastomers significantly.

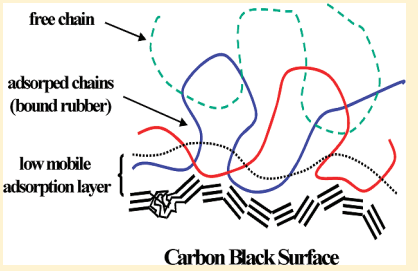

1. INTRODUCTION

Technical rubbers represent an important class of materials with a wide range of applications. The macroscopic properties of the rubbers can be strongly modified by compounding with plasticizers, fillers and other additives, by changing the cross-linking system and cross-linking conditions. The mechanical properties of rubbers are strongly improved by reinforcing with active fillers. The most frequently used filler in the rubber industry is carbon black. The most of carbon blacks are near-spherical particles of colloidal size fused mainly into particle aggregates. The processing behavior, the performance and appearance of the final rubber products are largely influenced by the type and the amount of filler, and by the dispersion in the rubber. Despite numerous investigations on carbon-black filled rubbers,[1−11] the molecular origin of the reinforcement effect is still under discussion. A number of factors contribute to the significant improvement of the rubber properties by the incorporation of active fillers. Among the most important factors, determining the rubber reinforcement, the following should be mentioned: strain amplification due to the filler volume effect, filler−filler networking and filler−rubber interactions.

Characterization of the glass-transition temperature (T_g) and the dynamics of polymer chains at solid surface have attracted a lot of attention during the last two decades. A number of studies have revealed various and sometimes even opposite effects of a solid on the dynamics of adsorbed polymer molecules.[12−16] In some cases, a decrease in molecular mobility in the proximity of solid surface is observed. In other cases, an increase or no change of molecular mobility upon chain adsorption was shown. "*It seems that the existing theories of T_g are unable to explain the range of behaviors seen at the nanometer size scale, in part because the glass transition phenomenon itself is not fully understood*".[11] This controversy and the lack of understanding of the dynamical heterogeneity of polymer chains on the surface of solids have various reasons. *First of all*, the polymer-solid interactions depend on the type of solid surfaces, the composition of the mixtures, the mixing procedure, the dispersion of the solid particles in the polymer matrix and the storage conditions of the mixtures after their preparation. *Second*, several types of interactions occur at the surface of solids and these various interactions affect the chain behavior at different time and length scales. *Finally*, various techniques for studying the immobilization of polymer chains at the surface of solids differ in the sensitivity to motional heterogeneity and to the time and length scales of chain dynamics investigated. It should be noted that at temperatures well above T_g, the dynamics of polymer chains spreads over a wide range of frequency and length scales.[17]

Received: April 15, 2011
Revised: May 19, 2011
Published: June 02, 2011

On the molecular scale, the mobility of chain fragments which are adjacent to a solid surface is largely determined by the local adhesive forces. As a result of the short-range of the adsorption interactions and the short length of the statistical segment of elastomers, the fraction of the chain segments, whose mobility is strongly influenced by the surface effects, is small. Therefore, the possibilities for investigating the mobility of polymers chains at the surfaces in a *direct* manner are rather limited. Just a few techniques can provide information about the physical properties and the amount of interface between the polymer matrix and the solid surface. This information can be obtained by studying model mixtures consisting of, for example, rubber with very large amount of filler, which are not of practical relevance.[18−23] These studies have shown that a thin layer of rubber, which is at the surface of silica or carbon black, is immobilized by chain adsorption. The estimated thickness of the immobilized layer, the rubber−filler interface, is in the range of two diameters of the monomer unit. Filler aggregates, which are covered by the interface, can be considered as multifunctional physical cross-links, which contribute to the total network density of the rubber matrix.[21,22] Traditionally, the physical rubber−filler network is characterized by the content of the apparent "bound" rubber, which is determined as the amount of unvulcanized rubber still adhering to the dispersed filler aggregates after extraction.[24] Since the amount of bound rubber is related to the surface area and the surface activity of the fillers, this phenomenon provides indirect proof of a multicontact chain adsorption at the filler surface. The formation and the strength of the physical network influence most mechanical properties of filled rubbers.[18,21]

One of the most powerful methods for the characterization of reinforced rubbers is solid-state NMR. The method is very sensitive to the nanoscale heterogeneity of materials,[25] and provides detailed information about the structure of the polymer network.[26] ^{1}H NMR transverse magnetization relaxation (T_2 relaxation) experiments were widely used for studying chain dynamics in filled rubbers.[26,27] Three types of chain fragments with different chain mobility were observed in carbon-black filled compounds using NMR methods: i.e., (1) chain fragments whose local mobility is largely hindered, *tightly bound* rubber at the filler surface or rubber−filler interface; (2) chain fragments outside of the immobilized interface whose large spatial scale mobility is restricted due to chain adsorption, *loosely bound* fraction of bound rubber or *network chains* which are formed due to physical rubber−filler interactions; (3) *free rubber* with a relatively low number or without adsorption network junctions or *extractable rubber*.[22,28] The degree of heterogeneity increases with increasing filler content irrespective of the filler nature.[29]

Two effects can complicate the interpretation of the NMR relaxation data in relation to the chain dynamics, namely, (1) the presence of free radicals on the surface of carbon black[30] and (2) the magnetic field gradients introduced by the filler particles associated with magnetic-susceptibility differences between the filler and the rubber.[31] However, the immobilization of chain fragments is observed in mixtures of polymers with silica's which do not contain free radicals.[18−21,32] Recently developed double-quantum (DQ) ^{1}H NMR experiments provide results which are free of the possible artifacts, since they directly probe the restrictions (anisotropy) of chain motions.[33−37] Therefore, DQ NMR can provide more reliable information about rubber−filler interactions as compared to the ^{1}H NMR T_2 relaxation methods.

In this study, the rubber−filler interactions, the network structure in carbon black filled EPDM and the corresponding stress−strain properties are studied by low-resolution solid-state ^{1}H NMR methods and by analysis of stress−strain curves using the dynamic flocculation model (DFM).[38] In order to establish the role of several factors on the reinforcement, a large series of samples with various types and amounts of carbon black and vulcanized with various levels of sulfur vulcanization packages was prepared for the study. The immobilization of EPDM chain fragments on the carbon black surface is studied by DQ NMR and spin-diffusion experiments. The network structure, which is formed by the chemical and physical network junctions, is analyzed by ^{1}H NMR T_2 relaxometry.[26] The mechanically active network density is determined using the DFM approach. A comparison of the network structure determined by NMR and the analysis of stress−strain curves allow better understanding of the reinforcement mechanisms.

2. EXPERIMENTAL SECTION

2.1. Sample Composition and Preparation. The following samples were prepared for the study: unfilled and carbon black filled EPDM compounds, carbon black with just bound EPDM, and unfilled and filled EPDM vulcanizates. The composition of compounds is provided in weight parts of component per hundred weight parts of the rubber (phr).

Preparation of Compounds. The EPDM grade K4802 from DSM Elastomers B.V. was used for preparation of all samples. This amorphous grade of EPDM rubber is composed of 48 wt % ethylene, propylene and 4.5 wt % 5-ethylidene-2-norbornene (ENB). The carbon blacks used were rubber-grade furnace blacks N550, N330, and N115 from Cabot Corporation. The specific surface area of these blacks, which was determined by the adsorption of hexadecyl trimethylammonium bromide (CTAB method), was 30, 83, and 142 m^2/gram, respectively. For various calculations performed below, densities of carbon black and EPDM of 1.8 and 0.854 g/cm^3, respectively, were used. The EPDM compounds were prepared on a laboratory two-roll mill (1 mm gap; 1:1.1 rotor speed ratio; 60 °C). First, the EPDM polymer was milled into a sheet and zinc oxide was mixed in. Next, the carbon black was added in small steps with the rubber sheet being cut and turned to ensure homogeneous mixing. The maximum amount of carbon blacks with higher specific surface area was lower. Then, the sulfur vulcanization chemicals were added together and mixed in. Finally, the compound was further homogenized with a mill gap of 0.5 mm. It was more difficult to achieve visually homogeneous compounds and, thus, the total mixing time was longer upon increasing the carbon black content in the series N550 < N330 < N115.

Preparation of a Bound Rubber Sample. When an elastomer and a reinforcing filler are mixed, part of the rubber cannot be extracted even after prolonged extraction in a good solvent. The residual carbon gel or silica gel mainly results from physical adsorption of rubber chains onto the filler particles, but also partly from a small amount of chemical cross-links and/or grafting of rubber chains onto the filler surface. The bound-rubber fraction is, by definition, the weight percent of nonextractable rubber relative to the total rubber in the compound before extraction. According to previous studies,[39,40] the amount of bound rubber depends on the storage time of the compounds prior to the extraction, the extraction time and temperature, and, to a small extent, the quality of the solvent used for the extraction.[22] The bound rubber sample was obtained as follows. The compound containing 60 phr of N115 carbon black was cut into approximately 1 mm^3 pieces. About 1 g of the compound was subsequently immersed in *o*-xylene and extracted for 30 days at room temperature. To prevent possible degradation and/or cross-linking, 0.1 wt % of 2,6-di-*tert*-butyl-*p*-cresol (DTPC) stabilizer was added to the solvent. The solvent with dissolved rubber was decanted every day in the first week of the extraction and fresh solvent

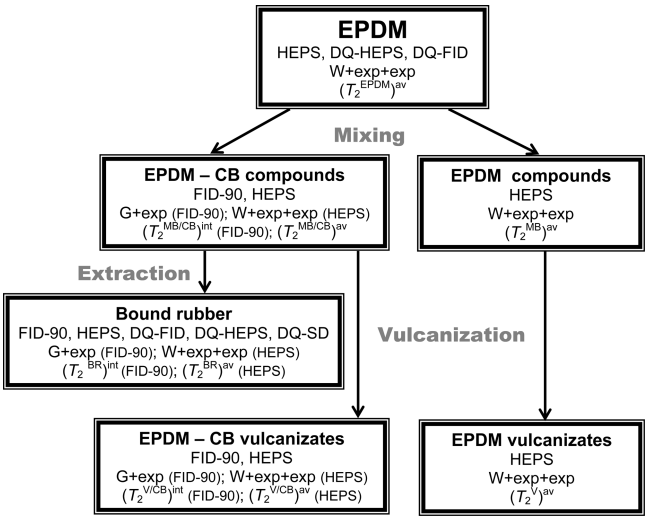

Figure 1. Samples studied, types of NMR experiments used, fitting functions used for the analysis of NMR T_2 relaxation decays, and NMR T_2 relaxation parameters obtained by the least-squares fit of T_2 decays. Abbreviations are explained in the Experimental Section.

was added. During the next 23 days of extraction, the solvent was replaced each third day. Finally, the residual (carbon black)/rubber gel was isolated and immersed in pentane for 4 days with one time solvent refreshment after 2 days. The filler/rubber gel was dried for 1 day in an oven at 60 °C in a vacuum of 5 mBar and a small nitrogen flush. The bound EPDM rubber sample contained 300 phr of carbon black N115.

Preparation of Vulcanizates. EPDM compounds with different amounts and types of carbon black were cross-linked using sulfur vulcanization. The compounds were vulcanized with three different levels of a sulfur-based package here referred to as 50%, 100%, and 200%. The 50% package was composed of 2.5 phr ZnO, 0.5 phr stearic acid, 0.31 phr mercaptobenzothiazole (MBT-80), 0.62 phr tetramethyluram disulfide (TMTD-80), and 0.94 phr sulfur S-80. The 100% and 200% samples were prepared with two and four times of these amounts, respectively. The compounds were vulcanized in a compression mold at 160 °C. The vulcanization time t_{90} was determined with a Monsanto to vulcameter. For uniaxial testing, axial-symmetrical dumbbells with 15 mm thickness were prepared in a specially designed mold.

2.2. NMR Experiments. ^{1}H NMR relaxation experiments were performed for static samples in 9 mm NMR tubes on a Bruker Minispec MQ-20 spectrometer operating at a proton resonance frequency of 20 MHz. The dead-time of the receiver and the duration of the 90°- and 180°-pulses were 7 μs, 2.8 and 5.3 μs, respectively. A BVT-3000 temperature controller was used for temperature regulation with an accuracy of ±0.1 °C. All experiments were performed at 90 °C.

The samples studied, the type of NMR experiments used, the fitting functions used for the analysis of the NMR T_2 relaxation decays, and the NMR T_2 relaxation parameters obtained are discussed below and summarized in Figure 1.

2.2.1. ^{1}H NMR Solid– and Hahn–Echo Experiments. Three types of NMR T_2 relaxation experiments have been performed for an accurate study of the mobile and immobilized fractions in filled EPDM.[22,42] The free induction decay (FID) of the bound rubber sample was measured using a 90°-pulse excitation (FID-90) and the solid–echo pulse sequence (FID-SEPS). The transverse magnetization relaxation of the mobile rubber matrix was measured in all samples by the Hahn–echo pulse sequence (HEPS).

Knowledge of the FID shape for the immobilized rubber fraction with a short T_2 relaxation time is required for the accurate deconvolution of the FID into the two components, corresponding to the immobilized and mobile rubber fractions. *The shape of the FID* for the immobilized fraction of the bound rubber was determined by the FID-SEPS: [90°$_x$ – τ_{se} – 90°$_y$ – τ_{se} – acquisition], with the time τ_{se} = 10 μs. The FID-SEPS was used to record the initial part of the transverse magnetization relaxation. The point in time from the beginning of the first pulse $t = 2\tau_{se} + t_{90}$ (at the echo maximum) was taken as zero, where t_{90} is the duration of the 90° pulse. This pulse sequence has the advantage of avoiding the dead time of the spectrometer, allowing the accurate measurement of the shape of the initial part of the FID. The analysis of the FID-SEPS has shown that the FID shape for the immobilized adsorption layer in the bound rubber sample is close to the Gaussian (G) one. It should be noted that the fraction of immobilized rubber can be underestimated in this experiment.[42]

The amount of the immobilized fraction and the chain mobility of this fraction, as defined by the T_2 value, were determined by the FID-90: [90°$_x$ – dead time – acquisition of the amplitude $A(t)$ as a function of time t after the 90° pulse]. At a signal-acquisition time longer than 150–200 μs, the amplitude of FID, which is recorded using the FID-90 and the FID-SEPS, is affected by the inhomogeneity of the magnetic field B_0 itself and the large inhomogeneity of B_0 within the sample volume, which arises from inhomogeneous magnetic susceptibility of the heterogeneous sample. Therefore, only the part of FID at times <200 μs was analyzed. This part of the FID was least-squares fitted with the following function:

$$A(t) = A_0^{int} \exp(-t/T_{2A}^{int})^2 + B_0^{m} \exp(-t/T_{2B}^{m}) + BL \quad (1)$$

The baseline value (BL) was determined in a separate experiment performed with an empty NMR tube. The transverse magnetization relaxation components with a short (T_2^{int}) and a long (T_2^{m}) characteristic decay time were assigned to the relatively immobile and mobile EPDM chain fragments, respectively. The amount of the immobilized chain fragments is calculated as $\%T_2^{int} = [A_0^{int}/(A_0^{int} + B_0^{m})] \times 100\%$. It cannot be excluded that $\%T_2^{int}$ could be underestimated, since some of the immobilized chains at the surface of the carbon black particles may not be detected as a result of the large shift of the resonance frequency and the relaxation effects combined with spin diffusion due to the paramagnetic impurities (free radicals) at the surface of the carbon black.

The FID experiment cannot be used for an accurate determination of T_2 relaxation times longer than about 100 μs, which are typical for EPDM rubbers.[22,36,41] Therefore, the HEPS [90°$_x$ – t_{He} – 180°$_y$ – t_{He} – acquisition of the amplitude of the echo maximum] was used to record the slow part of the T_2 relaxation decay for the mobile fraction, where the echo time (t_{He}) was varied between 35 μs and 400 ms. At $t_{He} \geq 35$ μs, the major part of the signal from the immobilized rubber decays nearly to zero. The HEPS makes it possible to eliminate the magnetic field and chemical shift inhomogeneities and to accurately measure the T_2 relaxation time for the mobile rubber fraction.[22]

A quantitative analysis of the shape of the T_2 decay for rubbers is not always straightforward, due to the complex origin of the relaxation function itself[43–48] and the structural heterogeneity of polymer networks.[21,22,26] Theoretical models describing the decay of the transverse magnetization relaxation (T_2 decay) for polymer melts and model networks cannot be used for the analysis of heterogeneous networks, if the type of heterogeneity is unknown. Since this is the case for the samples studied, a phenomenological approach was used in the present study. The T_2 decay, which was measured by the HEPS, was described with a linear combination of Weibull and two exponential functions:

$$A(t) = A_0[f_A \exp(-t/T_{2A})^{\alpha} + f_B \exp(-t/T_{2B}) + f_C \exp(-t/T_{2C})] \quad (2)$$

with α = 1.38 providing the best fit of the shape of the relaxation component with short T_2 value, and fractions f_A, f_B, and f_C for the components with relaxation times T_{2A}, T_{2B}, and T_{2C}, respectively. Rather than assigning specific types of network chains to the *A*, *B*, and

C components in eq 2, we extract from the decay an effective overall decay time $T_2^{index})^{av}$, which is determined as follows: $[(T_2^{index})^{av}]^{-1} = [f_A/T_{2A} + f_B/T_{2B} + f_C/T_{2C}]^{-1}$, where *index* designates the type of the sample (Figure 1). The $(T_2^{index})^{av}$ was used for determining the weight-average molar mass of the network chains. The random error of the $(T_2^{index})^{av}$ values was smaller than 2%. For estimating the systematic error caused by the fit model, we have used also other model shapes, such as a single Weibull (W) function, and a superposition of a Weibull and a single exponential functions. These approaches yielded $(T_2^{index})^{av}$ values within ~5% of the values obtained by use of eq 2.

2.2.2. ^{1}H NMR DQ Experiments. The proton DQ build-up (DQ-FID) curve was recorded using the pulse sequence $[90°_x - t_{ex} - 90°_{-x}]_{EX} - [t_{DQ}]_{EV} - [90°_y - t_{ex} - 90°_{-y}]_{RE} - t_z - [90°_x$ – acquisition of the amplitude $A(t)$ of the transverse magnetization$]_{DE}$. The subscripts EX, EV, RE, and DE stand for excitation, evolution, reconversion and detection periods, respectively. The z-filter time t_z was set to 5 ms, according to a previous NMR study of EPDM vulcanizates.[36] The initial amplitude $A(0)$ of the transverse magnetization relaxation was determined by a least-squares fit of the FID at different excitation times, t_{ex}. The four-pulse sequence does not compensate for resonance offsets and differences in the chemical shifts for the different types of hydrogen atoms are not compensated. Therefore, this pulse sequence was only used for a qualitative study of chain immobilization in filled EPDM samples.

2.2.3. ^{1}H NMR DQ-HEPS Experiments. DQ-filtered Hahn-echo experiments (DQ-HEPS) were carried out to confirm the immobilization of the rubber matrix in the bound EPDM rubber. The decay of the transverse magnetization relaxation of the mobile fraction of the rubbery matrix in the bound rubber sample and of the unfilled EPDM's was recorded using the DQ-HEPS pulse sequence: $[90°_x - t_{ex}/2 - 180°_x - t_{ex}/2 - 90°_{-x}]_{EX} - [t_{DQ}]_{EV} - [90°_y - t_{ex}/2 - 180°_y - t_{ex}/2 - 90°_{-y}]_{RE} - t_z - 90°_x - t_{He} - 180°_y - t_{He} -$ [acquisition of the amplitude $A(t)$ of an echo maximum]. The first part of the DQ-FID and DQ-HEPS pulse sequences, $[90°_x - t_{ex}/2 - 180°_x - t_{ex}/2 - 90°_{-x}]_{EX}$, excites DQ coherences. The t_{DQ} was set to 5 μs. The DQ coherences are converted by $90°_y$ and $90°_{-y}$ pulses to the z-polarization. The 180° refocusing pulses in the middle of the excitation and the reconversion periods eliminate the effects of resonance offsets and differences in the chemical shifts for different types of hydrogen atoms.[49] After the delay time t_z of the DQ filter, the HEPS was applied. The condition of selecting the isotropic powder average dipole−dipole interactions is broken for short DQ times. Simply, the magnetization of the segments with (residual) coupling tensors oriented along B_0 is enhanced, as compared to the other orientations, especially those at the magic angle. Therefore, a sufficiently long delay time t_z is required for proper redistribution of the magnetization between the chains with different direction of the end-to-end vector with respect to the B_0 direction. The redistribution of the magnetization is effective on distances that are comparable with the length scale of spin diffusion and/or translational chain mobility within time t_z. The time t_z was set to 5 ms, since the experiments with different t_z times have shown that 5 ms was sufficient for the redistribution of the magnetization over all rubbery chains either due to spin diffusion or large spatial-scale chain mobility.[36,50] Thus, by a proper choice of the excitation time, the decay of the transverse magnetization relaxation of rubbery chains of different length and, consequently, with different anisotropy of the chain motions, and the strength of the dipole−dipole interactions can be selected.[48,51−55]

2.2.4. ^{1}H NMR DQ-Filtered Spin Diffusion Experiments. Spin-diffusion experiments with a DQ dipolar filter were performed to answer the following question: is an immobilized adsorption layer present or not on the surface of carbon black? ^{1}H NMR spin-diffusion data were recorded by using the following pulse sequence: $[90^0_x - \tau_{ex} - 90^0_{-x} - t_{DQ} - 90^0_y - \tau_{ex} - 90^0_{-y} - t_d - 90^0_x -$ FID], where τ_{ex} and t_d are the excitation and the spin-diffusion times, respectively. An excitation time of 15 μs was used in the experiment. At this excitation time, the DQ filter selects mainly the signal from relatively immobile chain fragments in polymers.[34,35,53] The evolution time of the DQ coherences, t_{DQ}, was 5 μs in all experiments.

2.2.5. Determination of the Molar Mass of the Network Chains Which Are Formed by Chemical Cross-links and Physical Junctions. Different NMR methods with relatively basic or sophisticated characters can be used for investigating the network structure in rubbers. For the characterization of large series of samples, however, one should choose the most robust, convenient and accurate NMR method. ^{1}H NMR T_2 relaxometry is widely used for studying the network structure in rubbery materials.[26] The T_2 relaxation time is largely affected by the anisotropy of the chain motions, or more precisely, the residual dipolar couplings. The distinguishing feature of the T_2 relaxation for cross-linked polymers is the plateau, observed at temperatures that are well above T_g. The temperature-independence of T_2 at the plateau (T_2^{pl}) is attributed to constraints, which limit the number of the possible conformations of a network chain relative to those of a free chain. On the basis of Gaussian chain statistics, the theory of transverse magnetization relaxation in elastomeric networks relates T_2^{pl} to the number of statistical segments, Z, in the network chains that are formed by the chemical cross-links and the physical network junctions:[56,57]

$$Z = (T_2^{pl})/[a(T_2^{rl})] \quad (3)$$

where a is a theoretical coefficient, which depends on the angle between the segment axis and the internuclear vector for the nearest nuclear spins at the main chains. For polymers containing aliphatic hydrogen atoms in the main chain, this coefficient is close to 6.2 ± 0.7.[57] T_2^{rl} is the relaxation time measured below T_g for the polymer swollen in a deuterated solvent. T_2^{rl} for swollen EPDM measured at −133 °C is 10.4 ± 0.2 μs.[41] Using the number of backbone bonds in one statistical segment, designated C_∞, the weight-average molar mass of the network chains, M_w, can be calculated from the Z value:

$$M_w = ZC_\infty M_u/n \quad (4)$$

where M_u for EPDM is the average molar mass per elementary chain unit for copolymer chains (M_u = 34.7 g/mol for EPDM used in this study), and n = 2 is the number of backbone bonds in an elementary chain unit. A C_∞ value of 6.62 for an alternating ethylene-propylene copolymer[58] was used for the calculation of M_w of the EPDM network chains. It was shown that this NMR method provides reliable values of the density of chemical cross-links and chains entanglements in cross-linked EPDM rubbers.[41] Estimated relative and absolute errors of M_w are ~2% and ~15%, respectively.[41]

2.3. Stress−Strain Properties of Filled Rubbers. Fillers have a major effect on the stress−strain properties of rubbers, but so far the micromechanical effects of the fillers are not fully understood. The extension of rubber elasticity theory of polymer networks to filler-reinforced elastomers involves different effects and mechanisms, which have been discussed by a variety of authors, but in most cases only on a qualitative level. On the one hand, the addition of hard filler particles leads to a stiffening of the rubber matrix that can be described by a hydrodynamic strain amplification factor. On the other hand, the constraints introduced into the system by attractive polymer−filler couplings implies a decreased network entropy, resulting in a linear increase of the network free energy with the number of effective polymer−filler bonds. A further effect may result from the formation of filler clusters or a filler network, due to strong attractive filler−filler interactions. A typical feature of carbon black filled rubbers is the pronounced stress softening during quasi-static deformations, which is also termed the Mullins effect due to the extensive measurements carried out by Mullins.[59] Depending on the history of straining, e.g., the extent of previous stretching, the rubber material undergoes an almost permanent change that drastically alters the elastic properties and increases hysteresis. Most of the softening occurs in the first deformation and after a few deformation cycles the rubber approaches a steady state with a constant cyclic stress−strain behavior.

2.3.1. Stress−Strain Experiments. Quasi-static, uniaxial stress−strain measurements at a strain rate $\dot{\varepsilon} \approx 0.01$/s and at 22 °C were carried out

with dumbbells using a Zwick 1445 universal testing machine. For strain measurements, two reflection marks were placed at a distance of $l_0 \approx 15$ mm. In these measurements five cycles have been performed between a minimum and maximum strain, ε_{min} and ε_{max}, respectively, and then the strain has been increased successively from 5% to 10%, 20%, 30%, 40%, 60%, 80%, and 100% for ε_{max}, while ε_{min} was kept constant at 0%. The fifth up and down cycles have been considered for the fitting procedure, which are regarded to be equilibrium cycles.

2.3.2. Interpretation of the Stress–Strain Curves by the Dynamic Flocculation Model. In order to estimate the mechanically active network density, stress–strain curves of the rubbers were analyzed using the dynamic flocculation model (DFM).[36] This model combines well established concepts of rubber elasticity with a micromechanical approach of dynamic filler flocculation in strained rubbers at different elongations. The stress response of filled rubbers as a function of strain can be derived from the following mesoscopic phenomena. A successive breakdown of filler clusters takes place upon increasing the strain of an unconditioned, virgin rubber sample. This process begins with the largest filler clusters and continues up to a minimum cluster size. Upon decreasing the strain, complete reaggregation of the filler particles takes place. However, the filler–filler bonds, which are formed again after once being broken, are significantly weaker than in the virgin sample. At subsequent stress–strain cycles of a prestrained, reinforced sample, two micromechanical mechanisms can be distinguished: (i) hydrodynamic reinforcement of the rubber matrix by a fraction of rigid filler aggregates with strong virgin filler–filler bonds, which have not been broken during previous deformations; (ii) cyclic breakdown and reaggregation of the remaining fraction of more soft filler clusters with damaged and hence weaker filler–filler bonds. The fraction of rigid (unbroken) filler clusters decreases with increasing strain, while the fraction of soft filler clusters increases. The mechanical action of the soft filler clusters refers primarily to a viscoelastic effect, since any type of cluster that is stretched in the stress field of the rubber stores energy that is dissipated when the cluster breaks. This mechanism leads to a filler-induced viscoelastic hysteresis contribution to the total stress, which significantly affects the internal friction of the filled rubber samples. Note that this kind of hysteresis response is present also in the limit of quasi-static deformations, where no explicit time dependency of the stress–strain cycles is taken into account.

Accordingly, the apparent stress resulting in the DFM consists of two contributions: (i) the stress of the rubber matrix including hydrodynamic reinforcement, and (ii) the stress of the strained and broken filler clusters. The free energy density of filler reinforced rubber is given by

$$W(\varepsilon_\mu) = (1 - \Phi_{eff}) W_R(\varepsilon_\mu) + \Phi_{eff} W_A(\varepsilon_\mu) \tag{5}$$

with Φ_{eff} being the effective filler volume fraction of the structured filler particles, e.g., primary carbon black aggregates. The first addend considers the equilibrium energy density stored in the strained rubber matrix, which includes hydrodynamic strain amplification effects varying with the fraction of relatively stiff filler clusters with strong virgin filler–filler bonds. The second addend considers the energy stored in the residual fraction of more soft filler clusters with damaged bonds that are deformed in the stress field of the rubber matrix.

The free energy density of the strained rubber matrix is described by a nonaffine tube model of rubber elasticity:

$$W_R(\varepsilon_\mu) = \frac{G_c}{2}\left\{\frac{(\sum_{\mu=1}^{3}\lambda_\mu^2 - 3)\left(1 - \frac{T_e}{n_e}\right)}{1 - \frac{T_e}{n_e}(\sum_{\mu=1}^{3}\lambda_\mu^2 - 3)} + \ln\left[1 - \frac{T_e}{n_e}(\sum_{\mu=1}^{3}\lambda_\mu^2 - 3)\right]\right\} + 2G_e(\sum_{\mu=1}^{3}\lambda_\mu^{-1} - 3) \tag{6}$$

The first bracket term of eq 6 considers the interchain junctions, with an elastic modulus G_c proportional to the density of network junctions. The second addend is the result of tube constraints, whereby the tube constraint modulus G_e is proportional to the entanglement density of the rubber. The parenthetical expression in the first addend corresponds to a non-Gaussian extension of the tube model taking into account the finite chain extensibility of the polymer network. The finite extensibility parameter is chosen as the ratio n_e/T_e with n_e being the number of statistical chain segments between two successive entanglements and T_e is the trapping factor characterizing the portion of elastically active entanglements. Since T_e increases with the number of cross-links in the system ($0 < T_e < 1$), the finite extensibility parameter decreases with increasing cross-linking density.

The presence of rigid filler clusters, with bonds in the virgin, unbroken state of the sample, give rise to hydrodynamic reinforcement of the rubber matrix. This is specified by the strain amplification factor X, which relates the external strain ε_μ of the sample to the internal strain ratio λ_μ of the rubber matrix:

$$\lambda_\mu = 1 + X\varepsilon_\mu \tag{7}$$

In the DFM, the strain amplification factor depends on the preconditioning of the sample and gives rise to the well-known stress softening effect of filler reinforced rubbers. In the case of preconditioned samples and for strains smaller than the previous straining ($\varepsilon_\mu < \varepsilon_{\mu,max}$), the strain amplification factor X is independent of strain and determined by $\varepsilon_{\mu,max}$: $X = X(\varepsilon_{\mu,max})$. For the first deformation of virgin samples, it depends on the external strain $X = X(\varepsilon_\mu)$. For fractal clusters, $X(\varepsilon_{\mu,max})$ or $X(\varepsilon_\mu)$ can be evaluated by averaging over the size distribution of rigid clusters in all space directions. In the case of preconditioned samples, this yields:

$$X(\varepsilon_{\mu,max}) = 1 + c\Phi_{eff}^{2/3 - d_f}\sum_{\mu=1}^{3}\frac{1}{d}\left\{\int_0^{\xi_{\mu,min}}\left(\frac{\xi'_\mu}{d}\right)^{d_w - d_f}\phi(\xi'_\mu)\,d\xi'_\mu + \int_{\xi_{\mu,min}}^{\infty}\phi(\xi'_\mu)\,d\xi'_\mu\right\} \tag{8}$$

Here, c is a constant of order one, Φ_{eff} is the effective filler volume fraction, ξ_μ is the cluster size, d is the particle size, $d_f \approx 1.8$ is the mass fractal dimension and $d_w \approx 3.1$ is the anomalous diffusion exponent on cluster–cluster aggregation. $\phi(\xi_\mu)$ is the normalized size distribution that can be derived from the Smoluchowski equation of the kinetics of cluster–cluster aggregation of colloids. With the abbreviation $x_\mu \equiv \xi_\mu / d$ and the normalized mean cluster size $x_0 \equiv \xi_0/d$ it reads:

$$\phi(x_\mu) = \frac{4x_\mu}{x_0}\exp\left(-\frac{2x_\mu}{x_0}\right), \quad \mu = 1, 2, 3 \tag{9}$$

We point out that with this distribution function the integrals in eqs 8 and 10 can be solved analytically.

The second addend in eq 5 considers the energy stored in the substantially strained filler clusters. It delivers a filler induced hysteresis due to cyclic stretching, breakdown and reaggregation which is described by an integral over the soft filler clusters in stretching direction ($\dot{\varepsilon}_\mu > 0$) with strain dependent upper boundary:

$$W_A(\varepsilon_\mu) = \sum_{\mu}^{\dot{\varepsilon}_\mu > 0}\frac{1}{2d}\int_{\xi_{\mu,min}}^{\xi_\mu(\varepsilon_\mu)} G_A(\xi'_\mu)\varepsilon_{A,\mu}{}^2(\xi'_\mu, \varepsilon_\mu)\phi(\xi'_\mu)\,d\xi'_\mu \tag{10}$$

where the dot denotes time derivative. The sum over stretching directions with ($\dot{\varepsilon}_\mu > 0$) implies that clusters store energy by being stretched and reaggregate upon contraction. G_A is the elastic modulus and $\varepsilon_{A,\mu}$ is the strain of the soft filler clusters in spatial direction μ. The dependency of these quantities on cluster size ξ and external strain ε_μ can be derived from basic micromechanical considerations about elasticity and fracture mechanics of tender filler clusters imbedded into a strained rubber matrix. This also allows for a specification of the strain dependent integral boundaries $\xi_\mu = \xi_\mu(\varepsilon_\mu)$ and $\xi_{\mu,min} = \xi_{\mu,min}(\varepsilon_{\mu,max})$. A more detailed

dx.doi.org/10.1021/ma2007255 |*Macromolecules* 2011, 44, 4887–4900

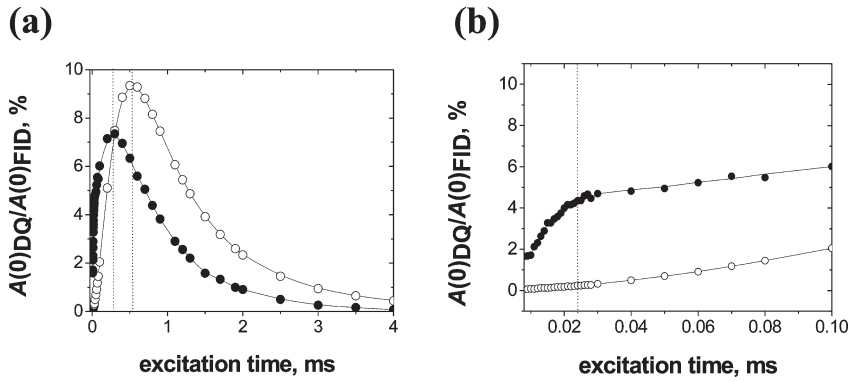

Figure 2. (a) Initial amplitude of free induction decay (FID) in the double quantum (DQ) experiment as a function of the excitation time (t_{ex}) for the bound rubber sample (closed circles) and the nonvulcanized EPDM without carbon black (open circles). The experiments are performed at 90 °C. The amplitude $A(0)_{DQ}$ is determined by a least-squares fit of the FID, which is recorded in the DQ-FID experiment. $A(0)_{DQ}$ is normalized to the initial amplitude of the transverse magnetization relaxation magnetization, $A(0)_{FID}$, which was determined by a least-squares fit of the FID measured without the DQ filter using the FID-90 experiment. (b) Expansion of the dependence at short excitation times showing the presence of a shallow maximum at ~25 μs, which is assigned to the immobilized EPDM at the carbon black interface. The bound rubber contains 300 phr carbon black N115. It is noted that the amplitude of the NMR signal in the DQ experiments should be smaller by at least 50% than its value measured without the DQ filter.

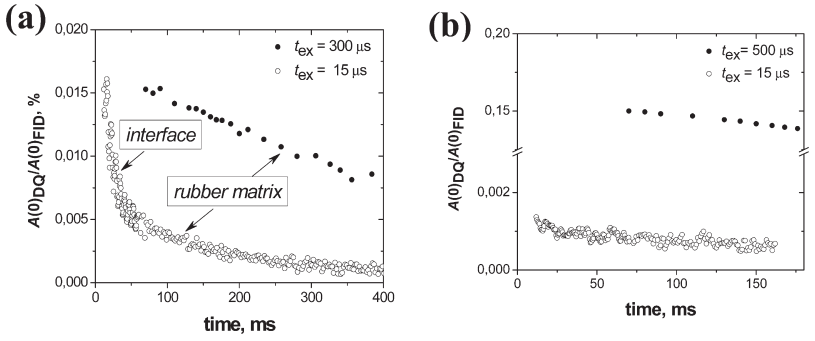

Figure 3. Transverse magnetization relaxation decays (T_2 decays) measured using DQ-FID and DQ-HEPS for (a) the bound rubber sample and (b) the nonvulcanized EPDM without carbon black. The DQ-FID and DQ-HEPS data are normalized to the initial amplitude of the FID for each sample, which is recorded using the FID-90 experiment. The experiments are performed at 90 °C.

physical description of the DFM and the various experimental tests of the model can be found in references 9 and 60−63.

3. RESULTS AND DISCUSSION

3.1. Chain Immobilization on the Carbon Black Surface. In the reinforced rubber vulcanizates the fraction of EPDM, which has direct interactions with the carbon black surface, is very small. Therefore, chain immobilization is studied for bound rubber sample, which contains 300 phr of carbon black N115 with high specific surface area. The amount of chains fragments, whose dynamics is affected by the filler surface in this bound rubber sample, should be high enough to be detected by low-resolution ^{1}H NMR methods.

Of the various NMR methods, ^{1}H NMR T_2 relaxometry is the most often used for studying rubber−filler interactions.[26] Although the method provides rather high selectivity to motional heterogeneity of filled rubbers, the results may be affected by microscopic magnetic susceptibility gradients caused by the filler particles,[64,65] and by free radicals at the carbon black surface.[21,66,67] In the spin−echo methods used in the present study, these artifacts are largely eliminated. Several NMR studies of silica and carbon black filled rubbers have provided convincing evidence for the presence of an immobilized polymer layer on the filler surface.[18,19,21,22,27,29,64,68] However, the existence of such an immobilized layer is still a matter of discussion.[13,69,70]

To enhance the selectivity of NMR to the motional heterogeneity of the filled EPDM samples, DQ NMR and NMR spin-diffusion methods are used in the present study. In the past decade, DQ and multi quantum (MQ) ^{1}H NMR experiments have provided detailed information about the structure of polymer networks,[31,32,34,35,71,72] and on the dynamic heterogeneity of the polymer chains grafted onto the silica surface.[35,73] Since the DQ method probes the strength of the dipole−dipole interactions, the method is free of the possible artifacts which were discussed above and could influence the interpretation of the T_2 relaxation results. Therefore, the DQ method can provide unambiguous information about the effect of EPDM−carbon black interactions on chain dynamics.

The initial amplitude of the FID in the DQ experiment is shown as a function of the excitation time (t_{ex}) for noncross-linked EPDM without carbon black and for the bound rubber sample (Figure 2). The DQ build-up curves show intensive maxima at approximately 500 and 300 μs for the unfilled and carbon-black bound EPDM, respectively. The position of the maximum (t_{max}) reflects constrains on large-spatial scale chain mobility in cross-linked EPDM rubbers.[34,74] A rubber with more restricted chain mobility (higher cross-link density) shows a DQ build-up maximum at shorter excitation time (t_{ex}). Fillers like carbon black also

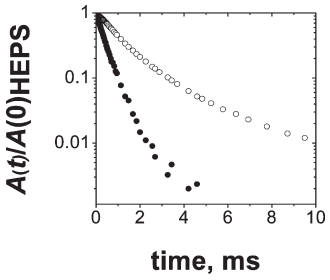

Figure 4. ^{1}H NMR transverse magnetization relaxation decay (T_2 decay) for nonvulcanized EPDM without carbon black and the bound rubber sample (open and closed circles, respectively). The decay was measured using the HEPS at 90 °C. Both decays are normalized to the initial amplitude of the magnetization as measured by the HEPS. It is noted that immobilized EPDM chain fragments at the surface of the carbon black in the bound rubber are not measured in this experiment.

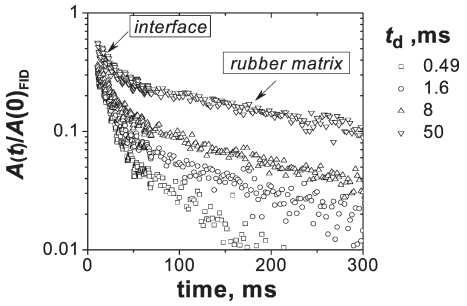

Figure 5. Free induction decay at different mixing time (t_d) in the spin-diffusion experiment for the bound rubber sample. The experiment is performed at 90 °C. Each decay is normalized to its initial amplitude which was determined by a least-squares fit of the decay using eq 1.

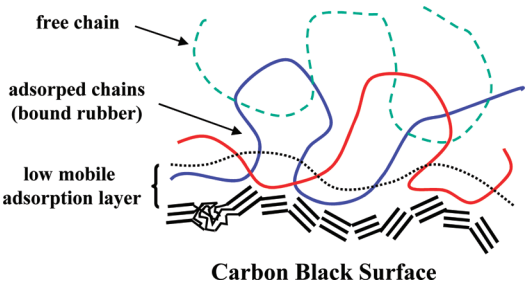

Figure 6. Simplified, graphic representation of EPDM chains at the carbon black surface. Parallel lines show graphite layers of carbon black nanocrystals. Low-mobile chain units adsorbed at the carbon black surface and mobile chain units outside of the rubber−filler interface are distinguished. The low-mobile chain fragments in the interface provide adsorption network junctions for the rubber matrix, explaining the origin of bound rubber. Free rubber chains in the bulk rubber (dashed line) have hardly any contacts with the surface of the carbon black and can be extracted from unvulcanized mixture by extraction with a good solvent.

constrain the chain mobility in the filler-attached rubber fraction. In addition to the shift of overall maximum in the DQ build up to shorter t_{ex} of ~300 μs, the bound rubber sample also show a weak shoulder at ~25 μs (Figure 2b). A DQ build-up maximum at such a short t_{ex} is typical for highly immobilized polymer chains, such as present in the crystal−amorphous interface of semicrystalline polymers,[55] and for short chain fragments, adjacent to the grafting sites on a silica surface.[35] Therefore, this shoulder at 25 μs is caused by strongly immobilized EPDM chains at the surface of carbon black. Since the maximum is observed at t_{ex} slightly larger than that for polymer chains in crystalline phases and glassy states,[34] the immobilized chain fragments are not fixed to the surface of the carbon black in a completely rigid way.

Two types of chain fragments with a large difference in chain mobility are also observed in the DQ-edited T_2 relaxation decays for filled EPDM in comparison to unfilled EPDM (Figure 3). The DQ-FID (t_{ex} = 15 μs) and the DQ-HEPS (t_{ex} = 300 and 500 μs) experiments are used to select the T_2 relaxation decays from either the immobilized or mobile fractions of bound rubber sample, respectively. At t_{ex} = 15 μs, the NMR signal from the immobile chain segments is mainly observed, whereas at t_{ex} = 300−500 μs the signal from mobile EPDM chains is detected.[34] The normalized amplitude of DQ-FID at t_{ex} = 15 μs is about 10 times smaller for the nonfilled EPDM than for bound rubber sample. Since a larger DQ signal intensity corresponds to a more restricted chain mobility, the mobility of some of the chain fragments in the bound rubber sample is strongly hindered. Contrary to the unfilled EPDM, the DQ-edited FID at t_{ex} = 15 μs for the bound rubber sample consists of two distinct components with a short and a long T_2 decay time. The two-component decay for the bound rubber sample provides additional proof of the large dynamic heterogeneity of the EPDM chains in the presence of carbon black.

The short and long T_2 values for these components are typical for the relaxation of rigid and soft materials, respectively. These relaxation components in the bound rubber are assigned to the low-mobile chain fragments at the rubber−filler interface and the viscoelastic chains in the rubber matrix, respectively. The relative amount of the rigid interface, which is determined by the analysis of the FID without the DQ filter, is 23 wt %. The HEPS experiment without the DQ filter for the nonfilled EPDM and the bound rubber sample reveals faster the T_2 relaxation for the bound rubber (Figure 4). Since rubbers with higher network density have shorter T_2,[26,34,37] mobility of the EPDM chain fragments in the rubbery matrix of the bound rubber sample is restricted due to chain anchoring at the filler surface.

The amount of the adsorption layer is very small in the carbon black compounds and filled EPDM vulcanizates, i.e., ≤ 1%, as follows from the FID-90 and the FID-SEPS experiments for these samples. Therefore, the high-modulus adsorption layer cannot provide large contribution to the modulus. However, there is a significant indirect effect of the interface. *First of all*, the physical network junctions at the EPDM - carbon black interface contribute to the total network density of the rubber matrix. *Second*, the EPDM-carbon black interactions significantly increase the energy required to breakdown the carbon black aggregates during deformation. *Finally*, the physical EPDM-carbon black junctions could dissipate energy during macroscopic deformation as a result desorption ↔ adsorption processes, which are enhanced at high local strains causing chain slippage along the filler surface. This results in higher homogeneity of the physical network.

3.2. Adsorption Layer and Rubber−Filler Network. Previous studies of carbon blacks have revealed a large energetic heterogeneity of the carbon black surface.[76,77] Two types of rubber chain immobilization can be considered, namely the formation of (1) "point-like" adsorption junctions at the high energy adsorption sites on the carbon black surface and (2) the presence of an immobilized adsorption layer covering the surface

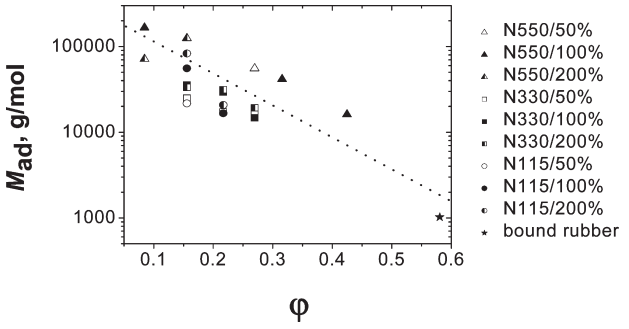

Figure 7. Weight-average molar mass between adsorption junctions along a chain (M_{ad}) as a function of the volume fraction of carbon black (φ) in the EPDM compounds and the bound rubber sample. Dotted line is a guide to the eyes.

of the carbon black. In the present study, an NMR spin-diffusion method is used for determining the type of chain immobilization. Figure 5 shows the FID's recorded at four different spin-diffusion times (t_d).

In this experiment, the magnetization of the immobilized rubber−filler interface is selected using the DQ filter. At short t_d, the fast decaying component, which originates from the immobilized layer, is mainly observed. At increasing t_d from 0.49 to 50 ms, the intensity of this component decreases, whereas the intensity of the component with a long decay time, associated with the mobile rubbery matrix, increases. This behavior is typical for heterogeneous polymers, which are composed of rigid and soft domains,[53] and it confirms that an immobilized rubber layer covers the surface of the carbon black. An estimation of the thickness of this layer requires several assumptions and a theoretical model describing the spin-diffusion process for this specific type of heterogeneous material. Quantitative analysis of the spin-diffusion data is out of the scope of the present study. Results, which are provided in section 3.1, are used for estimation of the interface thickness.

The thickness of the EPDM-carbon black interface in the bound rubber sample can be estimated from the composition of the bound rubber (25 wt % EPDM), the amount of the immobilized EPDM (23 wt %) and the specific surface area of the carbon black N115 (142 m^2/g). The thickness of the interfacial layer is estimated to be ∼0.6 nm assuming that the immobilized rubber forms a uniform layer covering all surface of the carbon black. As a result of carbon black agglomeration, not all surface of carbon black is available for polymer chain adsorption. Therefore, the thickness of the adsorption layer will be somewhat larger. Anyway, the estimated value is in a good agreement with that from the previous study of carbon black filled EPDM.[22] The small thickness of the immobilized adsorption layer is explained by the local origin of the surface field force of the carbon black and the short length of the statistical segment of the EPDM chains.

The average number of the backbone bonds per single adsorption junction $[(N_{C-C})^{ad}]$ can be estimated using the following equation[23,78]

$$\%(T_2^{BR})^{int} = (N_{C-C})^{ad} / [(N_{C-C})^{ad} + N_{phys}] \times 100\% \quad (11)$$

where N_{phys} is the average number of the backbone bonds between adjacent physical network junctions along the EPDM chains in the bound rubber sample. N_{phys} in the bound rubber sample equals ∼60 carbon−carbon bonds as will be shown in section 3.3.1. The calculated $(N_{C-C})^{ad}$ equals 18 C−C bonds per single adsorption junction.

It is anticipated that physical adsorption causes the flattening of the polymer chains at the carbon black surface. The length of 18 carbon−carbon bonds of an EPM chain in the *trans*−*trans* conformation is 2.35 nm. The crystallite edges on the carbon black surface with π-delocalized electrons are the sites for preferential chain adsorption having an enhanced adsorption energy of about 25 to 30 kJ/mol.[9] The average size of edges of graphite layers as estimated from X-ray diffraction,[79] neutron scattering,[80] and atomic force microscopy[81] is similar for all furnace carbon black grades and roughly equals 2.3 nm. This length is the same as $(N_{C-C})^{ad}$, indicating that the adsorbed EPDM chain fragments perfectly match the active carbon black crystallite edges. A morphological model for EPDM chains adjacent to the carbon black surface based on the results from the present study is shown in Figure 6.

3.3. Network Structure in Filled EPDM. The network structure in the rubbery matrix is largely affected by morphological and the molecular scale heterogeneity of filled rubbers, i.e., (i) the chemical heterogeneity of the unfilled rubbers, (ii) the morphological heterogeneity of a filled rubber due to the spatially heterogeneous distribution of the filler particles and their aggregation and agglomeration, (iii) the heterogeneous distribution of the chemical cross-links in the rubbery matrix, and (iv) the rubber−filler interface. The following types of network junctions are present in filled EPDM vulcanizates: chemical cross-links, EPDM−carbon black physical (adsorption) junctions, and finally temporary and trapped chain entanglements. The carbon-black surface could also restrict chain motions due to the excluded volume effect of the filler particles.[10,20,68,82] The contribution of the different types of network junctions to the total network density is estimated in the next sections.

3.3.1. The Molar Mass of the Network Chains in the Bound Rubber Sample. The filler aggregates, which are covered by the immobilized rubber interface, can be considered as multifunctional, physical cross-links, which provide network chains for the rubber matrix in the proximity of carbon black particles. The weight-average molar mass between the adsorption junctions along an EPDM chain in the bound rubber sample (M_{ad}) is determined from the relaxation time T_2^{ad}. T_2^{ad} is calculated from the T_2 values for the unfilled EPDM $(T_2^{EPDM})^{av}$ and the bound rubber sample $(T_2^{BR})^{av}$. It is assumed that the number of chain entanglements and the number of adsorption network junctions are additive to the network density and, thus, $(T_2^{ad})^{-1} = [(T_2^{BR})^{av}]^{-1} - [(T_2^{EPDM})^{av}]^{-1}$. Gaussian chain statistics is assumed for the calculation of M_{ad}, although it should be noted that the Gaussian characteristics of the elastomeric chains can be disturbed by the nonpenetrable filler particles in the rubber matrix. Because of this uncertainty, the calculated M_{ad} should be considered as an estimate. M_{ad} in the bound rubber sample amounts 1020 g/mol. This value is nearly two times smaller than the mean molar mass of the chain segments between chain entanglements in nonfilled EPDM, ∼1900 g/mol, and is significantly smaller than the molar mass between chemical cross-links in typical EPDM vulcanizates (∼1500−4000 g/mol).[41,74] The mean end-to-end distance between the adjacent adsorption junctions, which is calculated for Gaussian chains,[22] is in the same range as the mean distance between the carbon black aggregates in bound rubbers, i.e., 5−10 nm.[22,83] This suggests that there are chains, which are adsorbed on different carbon-black particles,

Table 1. Characteristics of Network Structure in Unfilled and Filled EPDM Vulcanizates[a]

carbon black			Ψ, m^2_{CB}/cm^3_{EPDM}	vulc, %	M_{ad}, g/mol	M_{chem}, g/mol	$(M_{tot})^{NMR}$, g/mol	$(1/2M_{chem})^{NMR}$, mmol/kg	$(1/2M_{tot})^{NMR}$, mmol/kg	$(1/2M_{tot})^{mech}$, mmol/kg
type	phr	φ								
	0	0	0	50	-	3880	1400	129	358	230
	0	0	0	100	-	2210	1100	226	454	282
	0	0	0	200	-	1810	1010	276	494	370
N550	20	0.0845	5.112	50	167 000	3970	1410	126	355	252
		0.0845	5.112	100	167 000	2500	1160	200	431	316
		0.0845	5.112	200	71 500	1870	1020	267	492	400
	40	0.156	10.25	50	125 000	4240	1430	118	351	304
		0.156	10.25	100	135 000	2230	1100	224	454	419
		0.156	10.25	200	130 000	1850	1020	270	491	494
	80	0.270	20.50	50	55 600	2510	1140	199	437	664
	100	0.316	25.52	100	41 700	2540	1140	197	437	924
N330	40	0.156	28.36	50	25 000	4310	1370	116	365	540
		0.156	28.36	100	35 700	2530	1140	198	440	654
		0.156	28.36	200	33 300	1830	988	273	506	721
	60	0.217	42.54	50	17 200	4310	1340	116	373	584
		0.217	42.54	100	29 400	2450	1110	204	449	781
		0.217	42.54	200	31 200	1740	968	288	522	901
	80	0.270	56.72	50	17 200	3970	1300	126	385	627
		0.270	56.72	100	14 700	2670	1100	187	449	752
		0.270	56.72	200	19 200	1830	967	273	517	938
N115	40	0.156	48.52	50	21 700	4310	1360	116	368	438
		0.156	48.52	100	55 500	2540	1150	197	434	583
		0.156	48.52	200	83 000	1630	943	307	530	703
	60	0.217	72.78	50	16 700	4310	1330	116	375	515
		0.217	72.78	100	16 700	2670	1130	187	444	634
		0.217	72.78	200	20 800	1800	945	278	529	857
N115[b]	300	0.581	364	-	1020	-	664			

[a] (a) The weight-average molar mass between chemical crosslinks (M_{chem}), between adjacent adsorption junctions along EPDM chains (M_{ad}), and between all types of network junctions in unfilled and filled EPDM vulcanizates $(M_{tot})^{NMR}$ as determined using the NMR T_2 relaxation method. (b) The weight-average network density originating from chemical crosslinks $[(1/2M_{chem})^{NMR}]$, the total network density as determined by the NMR method $[(1/2M_{tot})^{NMR}]$. The total network is composed of chemical crosslinks, adsorption junctions and chain entanglements. It is suggested that the entanglement density (M_{en}) is the same in all vulcanizates and equals 260 mmol/kg.[39] (c) The mechanically active network density $[(1/2M_{tot})^{mech}]$, which is determined by the analysis of stress-strain curves. The amount of carbon black is given in phr (weight parts of carbon black per hundred weight parts of rubber) and in the volume fraction of carbon black (φ). The maximum possible EPDM-filler contact area per unit volume of the rubber $[\Psi = (\varphi\rho S_{sp})/(1 - \varphi)]$ is also provided. The relative amount of the vulcanization package (vulc) is given in %. [b] Bound rubber.

and, in this way, these chains connect neighboring carbon-black aggregates in the filled rubbers.

3.3.2. The Effect of the Type of the Carbon Black on the Molar Mass of Network Chains Between Adsorption Junctions in EPDM Compounds. The structure of the physical network in carbon black filled EPDM is strongly heterogeneous as a result of the complex morphology of the carbon black filled rubbers. This causes a spatially heterogeneous or "bimodal"-like distribution of adsorption junctions in the rubber matrix of the filled EPDM.[22] The structure of the physical network consists of (1) a dense physical network in the bound rubber fraction, and (2) entangled free rubber chains with hardly any adsorption junctions. The amount of bound rubber fraction decreases with decreasing amount of carbon black and its specific surface area.[22]

The mean molar mass of the chain fragments between adjacent adsorption junctions in the EPDM − carbon black compounds is determined similarly to that in the bound rubber sample (section 3.3.1). The volume-average transverse relaxation time T_2 in heterogeneous networks provides the weight-average molecular mass of network chains since the contribution of network chains of different length to $(T_2^{MB/CB})^{av}$ is proportional to their molecular mass. Therefore, the value T_2^{ad} in filled EPDM is still largely determined by the free rubber fraction, which is not directly bound to the carbon-black surface.

The effect of the type and the amount of carbon black on M_{ad} is shown in Table 1, and in Figures 7 and 8. M_{ad} in the compounds decreases upon (1) increasing the volume fraction of the carbon black, φ, in the compounds and (2) increasing the maximum possible EPDM-filler contact area per unit volume of the rubber, $\psi = \varphi\rho S_{sp}/(1 - \varphi)$, where ρ and S_{sp} is the density and the specific surface area of carbon blacks, respectively. If the entire surface of the carbon black would be available for the adsorption of EPDM chains and the surface structure of different carbon blacks would be the same, then one would expect the same M_{ad} value for samples with the same ψ value regardless the type of carbon black. M_{ad} is slightly smaller for compounds filled

dx.doi.org/10.1021/ma2007255 |*Macromolecules* 2011, 44, 4887–4900

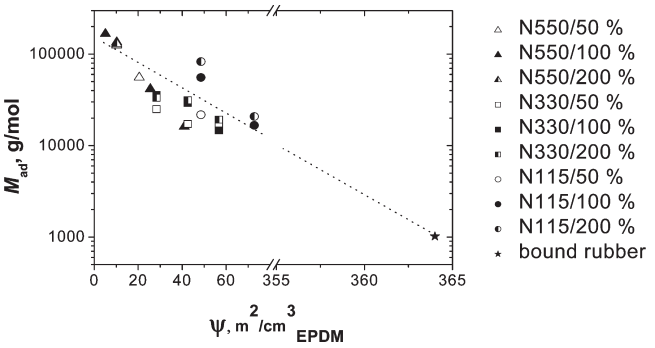

Figure 8. Weight-average molar mass between adsorption network junctions (M_{ad}) as a function of the maximum possible EPDM-carbon black contact area per unit volume of the rubber $[\Psi = (\varphi\rho S_{sp})/(1-\varphi)]$ in the EPDM compounds and the bound rubber sample. Dotted line is a guide to the eyes.

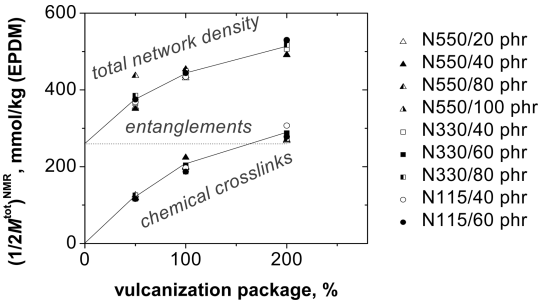

Figure 9. Volume-average network density as a function of the amount of vulcanization package in carbon black filled vulcanizates $[(1/2M_{tot})^{NMR}]$. The network is composed of chemical cross-links, adsorption junctions and chain entanglements. The contributions of chemical cross-links $(1/2M_{chem})^{NMR}$ and chain entanglements to $(1/2M_{tot})^{NMR}$ are also shown. Lines are guides to the eyes. The entanglement density in EPDM vulcanizates of ~260 mmol/kg was determined previously.[41]

with the carbon black having lower specific surface area (Figure 8). This can be caused by smaller agglomeration of carbon black in these compounds.

3.3.3. Molar Mass of the Network Chains Between Chemical Cross-Links in the EPDM Vulcanizates. The weight-average molar mass between chemical cross-links (M_{chem}) in unfilled and filled EPDM is calculated from T_2^{chem} relaxation time. T_2^{chem} is determined from the decrease in the T_2 value upon vulcanization, assuming additivity of all types of network junctions: $(T_2^{chem})^{-1} = [(T_2^{V})^{av}]^{-1} - [(T_2^{MB})^{av}]^{-1}$ and $(T_2^{chem})^{-1} = [(T_2^{V/CB})^{av}]^{-1} - [(T_2^{MB/CB})^{av}]^{-1}$ for unfilled and filled vulcanizates, respectively (for definition T_2^{index} see Figure 1). The weight-average density of the chemical cross-links $(1/2M_{chem})$ is shown as a function of the sulfur level for the different carbon black loadings in Figure 9. At a constant level of sulfur vulcanization package, the cross-link density is hardly affected by the type and the amount of carbon black, which indicates the absence of any effect of carbon black on the sulfur vulcanization efficiency of EPDM. The cross-link density is higher at higher amounts of the vulcanization package, as expected. The density of the chemical cross-links is comparable with the EPDM entanglement density at the largest amount of the

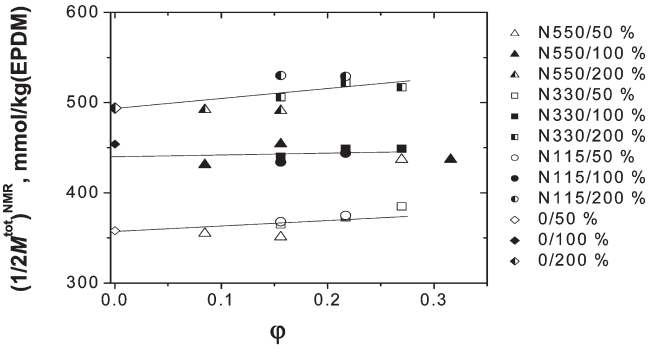

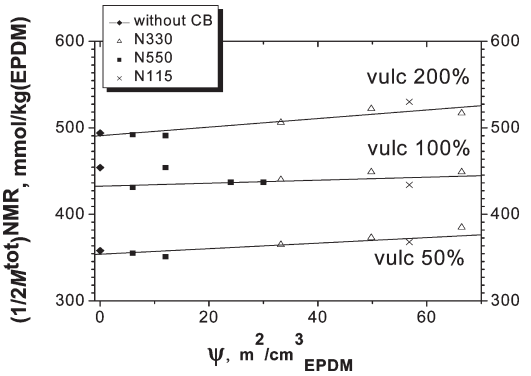

Figure 10. Volume-average network density in carbon black filled EPDM vulcanizates $[(1/2M_{tot})^{NMR}]$ at three different levels of vulcanization package: (a) $[(1/2M_{tot})^{NMR}]$ as a function of the volume fraction of carbon black (φ); (b) $[(1/2M_{tot})^{NMR}]$ as a function of the maximum possible EPDM−carbon black contact area per unit volume of the rubber $[\Psi = (\varphi\rho S_{sp})/(1-\varphi)]$ Lines are guides to the eyes. The network density is determined by the NMR T_2 relaxometry.

vulcanization package. A previous NMR T_2 relaxation and FT-Raman spectroscopy study of gum stock EPDM sulfur vulcanizates has shown that the average sulfur cross-link consists of approximately 2.8 sulfur atoms.[84] For 4.5% ENB-EPDM, most of the ENB is consumed upon vulcanization with amount of sulfur vulcanization package at approximately 200%. Therefore, the density of the chemical cross-links approaches a constant value at the level of sulfur vulcanization package higher than 100%, since the majority of ENB is consumed due to the reaction with sulfur.

3.3.4. The Total Network Density in Filled EPDM Vulcanizates by NMR. The total average network density $[(1/2M_{tot})^{NMR}]$, which is composed of chemical cross-links, chain entanglements and adsorption junctions, is calculated for unfilled and filled vulcanizates from the NMR $[(T_2^{V})^{av}]$ and $[(T_2^{V/CB})^{av}]$ relaxation times, respectively (Table 1, and Figures 9 and 10). Again, additivity of all types of network junctions to the total network density and, consequently, to the rate of the transverse magnetization relaxation is assumed. The network density is calculated assuming that the functionality of all types of network junctions equals four: $1/[(f/4)(M_{tot})^{NMR}]$, where f is the functionality of the network junctions. This assumption is certainly valid for unfilled sulfur EPDM vulcanizates.[41]

The data in Figures 9 and 10 show that the total network density is hardly affected by the type and the amount of the carbon black. This suggests a small contribution of the physical EPDM − carbon black junctions to the total cross-link density. But, it should be mentioned that the functionality of the adsorption junctions is unknown and can differ from four. Therefore, the

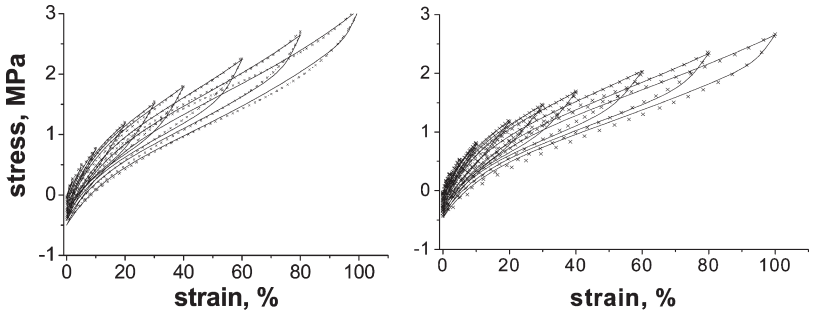

Figure 11. Uniaxial stress−strain cycles of EPDM vulcanizates filled with 60 phr carbon black N330 (left) and N115 (right). The lines show the fits of the stress−strain dependence using the dynamic flocculation model.[9]

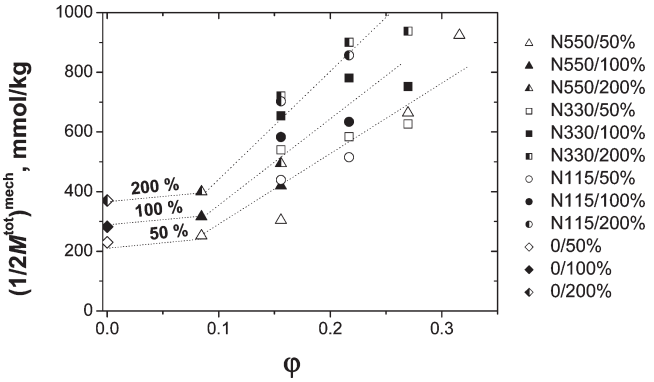

Figure 12. Mechanically active network density in the carbon black filled EPDM vulcanizates $[(1/2M_{tot})^{mech}]$ as a function of the volume fraction of carbon black (φ). Dotted lines are guides to the eyes, showing the effect of different levels of vulcanization package. The network density is determined by analysis of the stress−strain curves using the dynamic flocculation model.[9]

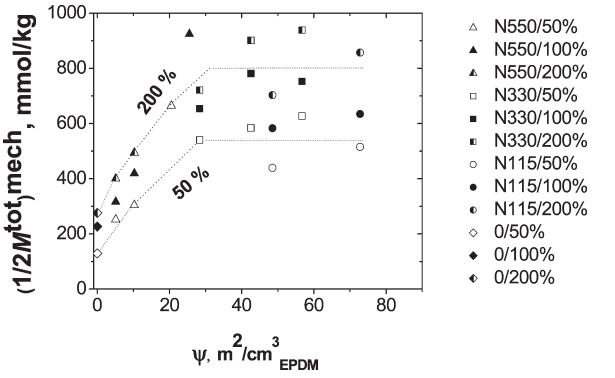

Figure 13. Mechanically active network density in the carbon black filled EPDM vulcanizates $[(1/2M_{tot})^{mech}]$ as a function of the maximum possible EPDM-carbon black contact area per unit volume of the rubber $[\Psi = (\varphi\rho S_{sp})/(1 - \varphi)]$. Dotted lines are guides to the eyes, showing the effect of different levels of vulcanization package. The network density is determined by analysis of the stress−strain curves using the dynamic flocculation model.[9]

total network density, as measured by the NMR method for filled rubbers, will suffer from an error, especially at high filler loadings and high specific surface area of the carbon black.

3.4. Stress−Strain Properties and Reinforcement Mechanisms. Figure 11 shows the experimental stress−strain cycles of the EPDM samples filled with 60 phr of N330 and N115 and cured at low level of sulfur vulcanization package, together with the best fits using the dynamic flocculation model. The tube-constrain modulus G_e = 0.6 MPa is calculated from the dynamic plateau modulus of the EPDM melt and is kept constant for all fits. The prefactor c = 2.5/3 of the hydrodynamic strain amplification factor is chosen according to the Einstein-relation and is also constant in all fits. For both samples, fair agreement between the fits and the measured cycles up to 100% strain is observed. The obtained fitting parameters listed in the graphs appear physically reasonable. Looking first at the filler specific parameters, it is found that the tensile strength of the virgin and damaged filler−filler bonds (s_v and s_d, respectively) and also the related mean cluster size (x_0 normalized by the particle size) is larger for the more active carbon black N115 with a higher specific surface area. The effective filler volume fraction (Φ_{eff}) is almost equal for both carbon blacks. The cross-link modulus (G_c) and, hence, the mechanically effective cross-link density is somewhat lower for the EPDM vulcanizates filled with carbon black N115. The finite extensibility parameter of the polymer network (n), describing the upturn of the stress−strain curves at large strain, is difficult to fit and found to be quite large for both samples due to the low vulcanization level.

The total mechanically active network density $[(1/2M_{tot})^{mech}]$ is calculated from the cross-link modulus G_c of carbon black filled EPDM. $(1/2M_{tot})^{mech}$ increases upon increasing the amount of the vulcanization package and increasing the volume fraction of carbon black (φ), as expected (Figure 12). At the same carbon black loading, no significant effect of the type of the filler is observed as follows from the data shown in Figure 13. The increase in the maximum possible EPDM-carbon black contact area per unit volume of the rubber (ψ) hardly influences $(1/2M_{tot})^{mech}$, which was also concluded from the NMR data discussed is section 3.3.4. This indicates that at high filler loadings the maximum possible EPDM-carbon black contact area is not achieved probably due to dispersion problems. At low ψ values the mechanically effective network density depicted in Figure 13 increases first but levels out at high ψ values because the filler particles in non dispersed agglomerates contact each other and a high amount of filler surface is not in contact with the polymer.

The total network density, as determined by NMR $[(1/2M_{tot})^{NMR}]$, is significantly lower than that determined from the stress−strain experiments $(1/2M_{tot})^{mech}$ for almost all filled samples, however it is larger for all three unfilled samples (Figure 14). Obviously, in contrast to the mechanical estimates, no pronounced effect of the constraints introduced by the filler on the total NMR network density is found. It should be noted

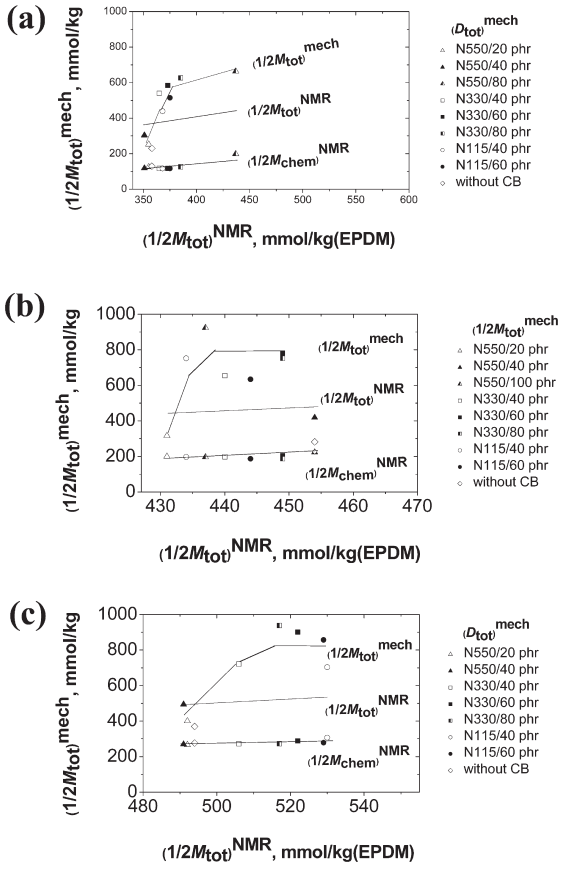

Figure 14. $(1/2M_{tot})^{mech}$ and $(1/2M_{chem})^{NMR}$ against $(1/2M_{tot})^{NMR}$ for vulcanizates with levels of vulcanization package 50% (a), 100% (b), and 200% (c). Lines are guides to the eyes.

that the density of adsorption junction, which is determined by NMR, is calculated suggesting their functionality equals four. If each of carbon black aggregates with adsorbed chains behaves under mechanical load as a single adsorption junction, the contribution of adsorption functions to the total NMR network density is underestimated. The dominating contribution to the mechanically active network density is provided by chemical cross-links and trapped chain entanglements in the EPDM rubber matrix because of relative low amount of strongly adsorbed chain segments. On the other side, the adsorption of chains at the filler surface impacts significantly the mechanical response of the composites even at high extension. This makes clear that the coupling of chains to the filler surface remains fixed also at large strain values. This coupling is not affecting the T_2-time which appears to be dominated by the rubber matrix. The effect of polymer−filler coupling on T_2 becomes visible in interphase-rich systems, only, e.g., the bound rubber samples (Figure 4). Here, the strong coupling of the chains to the filler decreases the T_2-time significantly indicating a high amount of short chain loops with the ends adsorbed at the filler surface.

4. CONCLUSIONS

Despite numerous investigations on polymer chains at solid surfaces and in filled rubbers using different techniques, the molecular origin of the reinforcement is still under dispute. This is partly related to the complexity of the phenomenon, since several mechanisms and several types on interactions and morphological heterogeneities in a large range of length scales play a role. Moreover, the structural heterogeneity of filled rubbers causes a large heterogeneity of the local stress−strain characteristics,[85] and, as a result, the interpretation of viscoelastic properties of heterogeneous networks is also not straightforward. Several reinforcing factors have been suggested in the literature. The most important ones are the following: (i) a hydrodynamic effect due to the volume occupied by the filler, (ii) an elastically active network of carbon black particles, and (iii) the formation of a layer of immobilized polymer at the surface of the carbon black particles.

To obtain a better understanding of the origin of reinforcement of rubbers by active fillers, a large series of nonfilled and carbon black filled EPDM vulcanizates was studied using solid-state NMR and mechanical testing. Advanced NMR relaxation experiments unambiguously show strong immobilization of EPDM chain fragments on the surface of carbon black. Results suggest that the adsorbed EPDM chain fragments perfectly match to carbon black crystal edges, which are active adsorption sites. The thickness of the immobilized EPDM − carbon black interfacial layer is estimated to be ≥0.6 nm. The amount of the adsorption layer is very small in the filled EPDM vulcanizates even at high loading and at high specific surface area of the carbon black. Therefore, direct impact of this immobilized layer on physical properties is expected to be small. An indirect effect of this adsorbed layer will be due to the formation of physical junctions that form a quasi-permanent network in the rubber matrix in the proximity of the carbon black aggregates. Because of the strong physical adsorption of the rubber chains onto the filler surface, the filler particles are "glued" in the rubber matrix and bridge adjacent carbon black aggregates. Although, the number of these adsorption junctions is significantly smaller than the density of the chemical cross-links and the chain entanglements, this physical network may help in redistribution of the local strains during deformation due to slippage of the physical junctions along the carbon black surface. The bridging chains increase energy required for the breakdown of carbon black aggregates and provide a source for dissipation of energy because of filler aggregate breakdown and reaggregation during deformation.

A microstructure-based model of stress-softening and filler-induced hysteresis has been applied to describe the quasi-static stress−strain behavior of filled rubbers under successive extension up to large strain. Besides the strongly nonlinear rubber elasticity, the model reproduces the filler-induced effects, i.e., strain amplification, stress softening and hysteresis in fair agreement with the experimental data. Generally, the fitted parameters lie in a physically reasonable range and can be interpreted in the frame of physically well understood quantities. The model has been used for the evaluation of the mechanically effective network density of reinforced elastomers, which increases with the amount of filler. It has been shown that the adsorption of chains impacts the mechanical response of the composites even up to high extension, demonstrating that the coupling of chains to the filler surface plays a major role in rubber reinforcement.

AUTHOR INFORMATION

Corresponding Author

*Corresponding author. E-mail: victor.litvinov@dsm.com.

ACKNOWLEDGMENT

This work was part of the research program of the Dutch Polymer Institute (DPI Project No. 511). The authors thank DPI

and DSM Resolve for financial support, and Roger Timmermans for preparing EPDM compounds.

REFERENCES

(1) Kraus, G. In *Reinforcement of Elastomers*; Wiley: New York, 1965.
(2) Donnet, J. B.; Voet, A. *Carbon Black Physics, Chemistry and Elastomer Reinforcement*; Marcel Dekker; New York, 1976.
(3) Rigbi, Z. *Adv. Polym. Sci.* **1980**, *36*, 21.
(4) Danneberg, E. M. *Rubber Chem. Technol.* **1975**, *48*, 410.
(5) Donnet, J. B.; Vidal, A. *Adv. Polym. Sci.* **1986**, *76*, 103.
(6) Edwards, D. C. *J. Mater. Sci.* **1990**, *25*, 4175.
(7) Heinrich, G.; Klüppel, M. *Adv. Polym. Sci.* **2002**, *160*, 1.
(8) Leblanc, J. L. *Prog. Polym. Sci.* **2002**, *27*, 627.
(9) Klüppel, M. *Adv. Polym. Sci.* **2003**, *164*, 1.
(10) Vilgis, T. *Polymer* **2005**, *46*, 4223.
(11) Allegra, G.; Raos, G.; Vacatello, M. *Prog. Polym. Sci.* **2008**, *33*, 683.
(12) Alcoutlabe, M.; McKenna, G. B. *J. Phys. Cond. Matter* **2005**, *17*, R461.
(13) Robertson, C. G.; Roland, C. M. *Rubber Chem. Technol.* **2008**, *81*, 506.
(14) Liu, Y.; Russell, T. P.; Samant, M. G.; Stöhr, J.; Brown, H. R.; Cossy-Favre, A.; Diaz, J. *Macromolecules* **1997**, *30*, 7768.
(15) Forrest, J. A.; Dalknoki-Veress, K.; Dutcher, J. R. *Phys. Rev. E* **1997**, *56*, 5705.
(16) Porter, C. E.; Blum, F. D. *Macromolecules* **2000**, *33*, 7016.
(17) Kimmich, R.; Fatkullin, N. *Adv. Polym. Sci.* **2004**, *170*, 1; and refs. therein.
(18) Litvinov, V. M. *Polym. Sci. USSR* **1988**, *30*, 2250.
(19) Litvinov, V. M.; Spiess, H. W. *Makromol. Chemie* **1991**, *192*, 3005.
(20) Kirst, K. U.; Kremer, F.; Litvinov, V. M. *Macromolecules* **1993**, *26*, 975.
(21) Litvinov, V. M. In *Organosilicon Chemistry II. From Molecules to Materials*; Auner, N.; Weis, J., Eds.; Wiley-VCH: Weinheim, Germany, 1996; pp 779−814.
(22) Litvinov, V. M.; Steeman, P. A. M. *Macromolecules* **1999**, *32*, 8476; and references therein.
(23) ten Brinke, J. W.; Litvinov, V. M.; Wijnhoven, J. E. G. J.; Noordermeer, J. W. M. *Macromolecules* **2002**, *35*, 10026.
(24) Danneberg, E. M. *Rubber Chem. Technol.* **1975**, *48*, 410.
(25) Schmidt-Rohr, K.; Spiess, H. W. *Multidimensional Solid-State NMR and Polymers*; Academic Press: London, 1994.
(26) Litvinov, V. M.; De, P. P., Eds.; *Spectroscopy of Rubbers and Rubbery Materials*; RAPRA Technology: Shawbury, U.K., 2002.
(27) Litvinov, V. M. In *Spectroscopy of Rubbers and Rubbery Materials*; Litvinov, V. M.; De, P. P., Eds.; RAPRA Technology: Shawbury, U.K., 2002; p 353 and references therein.
(28) Kenny, J. C.; McBrierty, V. J.; Rigbi, Z.; Douglass, D. C. *Macromolecules* **1991**, *24*, 436 and references therein.
(29) Moldovan, D.; Fechete, R.; Demco, D. E.; Culea, E.; Blümich, B.; Herrmann, V.; Heinz, M. *Macromol. Chem. Phys.* **2010**, *211*, 1579.
(30) McBrierty, V. J.; Kenny, J. C. *Kautsch. Gummi Kunstst.* **1994**, *47*, 342 and references therein.
(31) Leu, G.; Liu, Y.; Werstler, D. D.; Cory, D. G. *Macromolecules* **2004**, *37*, 6883.
(32) Papon, A.; Saalwächter, K.; Schäler, K.; Guy, L.; Lequeux, F.; Montes, H. *Macromolecules* **2011**, *44*, 913.
(33) Graf, R.; Demco, D. E.; Hafner, S.; Spiess, H. W. *J. Chem. Phys.* **1997**, *106*, 885.
(34) Schneider, M.; Gasper, L.; Demco, D. E.; Blümich, B. *J. Chem. Phys.* **1999**, *111*, 402.
(35) Wang, M.; Bertmer, M.; Demco, D. E.; Blümich, B.; Litvinov, V. M.; Barthel, H. *Macromolecules* **2003**, *36*, 4411.
(36) Litvinov, V. M. *Macromolecules* **2006**, *39*, 8727.
(37) Saalwächter, K. *Prog. Nucl. Magn. Reson. Spectrosc.* **2007**, *51*, 1.
(38) Klüppel, M.; Heinrich, G. *Rubber Chem. Technol.* **1995**, *68*, 623.
(39) Wolf, S.; Wang, M. J.; Tan, E. H. *Kautsch. Gummi Kunstst.* **1994**, *47*, 780.
(40) Danneberg, E. M. *Rubber Chem. Technol.* **1986**, *59*, 512.
(41) Litvinov, V. M.; Barendswaard, W.; Duin van, M. *Rubber Chem. Technol.* **1998**, *71*, 105.
(42) Litvinov, V. M.; Penning, J. P. *Macromol. Chem. Phys.* **2004**, *205*, 1721.
(43) Cohen-Addad, J. P. *Progr. NMR Spectroscopy* **1993**, *25*, 1.
(44) Cohen-Addad, J. P. In *Spectroscopy of Rubbery Materials*; Litvinov, V. M., De, P. P., Eds.; RAPRA Technology: Shawbury, U.K., 2002; p 291.
(45) Brereton, M. G. *Macromolecules* **1990**, *23*, 1119.
(46) Brereton, M. G. *Macromolecules* **1991**, *24*, 2068.
(47) Cohen-Addad, J. P.; Girard, O. *Macromolecules* **1992**, *25*, 593.
(48) Kulagina, T. P.; Litvinov, V. M.; Summanen, K. T. *J. Polym. Sci., Part B: Polym. Phys.* **1993**, *31*, 241.
(49) Munowitz, M.; Pines, A. In *Advances in Chemical Physics: Principles and Applications of Multiple-Quantum NMR*; Wiley Inter-Science: New York, 1987, Vol 66, p 1.
(50) Saalwächter, K.; Ziegler, P.; Spyckerelle, O.; Haidar, B.; Vidal, A.; Sommer, J. U. *J. Chem. Phys.* **2003**, *119*, 3468.
(51) Ba, Y.; Ripmesster, J. A. *J. Chem. Phys.* **1998**, *108*, 8589.
(52) Buda, A.; Demco, D. E.; Bertmer, M.; Blümich, B.; Reining, B.; Keul, H.; Höcker, H. *Solid State Nucl. Magn. Reson.* **2003**, *24*, 39.
(53) Buda, A.; Demco, D. E.; Blümich, B.; Litvinov, V. M. *ChemPhysChem* **2004**, *5*, 876.
(54) Cherry, B. R.; Fujimoto, C. H.; Cornelius, C. J.; Alam, T. M. *Macromolecules* **2005**, *38*, 1201.
(55) Hedesiu, C.; Kleppinger, R.; Demco, D. E.; Adams Buda, A.; Blümich, B.; Remerie, K.; Litvinov, V. M. *Polymer* **2007**, *48*, 763.
(56) Gotlib, Y. Y.; Lifshits, M. I.; Shevelev, V. A.; Lishanskii, I. A.; Balanina, I. V. *Polym. Sci. USSR* **1976**, *18*, 2630.
(57) Fry, C. G.; Lind, A. C. *Macromolecules* **1988**, *21*, 1292.
(58) Richter, D.; Farago, B.; Butera, R.; Fetters, L. J.; Huang, J. S.; Ewen, B. *Macromolecules* **1993**, *26*, 795 and references therein.
(59) Mullins, L. In *Reinforcement of Elastomers*; Kraus, G.; Ed.; Interscience Publ.: New York, London, and Sydney, 1965.
(60) Lorenz, H.; Meier, J.; Klüppel, M. In *Elastomer Friction: Theory, Experiment and Simulation. Lecture Notes in Applied and Computational Mechanics*; Besdo, D.; Heimann, B., Klüppel, M., Kröger, M., Wriggers, P., Nackenhorst, U., Eds.; Springer: Berlin, Heidelberg, Germnay, and New York, 2010; Vol. 51, p 27.
(61) Klüppel, M.; Heinrich, G. *Kautsch. Gummi Kunstst.* **2005**, *58*, 217.
(62) Lorenz, H.; Freund, M.; Juhre, D.; Ihlemann, J.; Klüppel, M. *Macromol. Theory Simul.* **2010**, *19*, 110.
(63) Vilgis, T. A.; Heinrich, G.; Klüppel, M. *Reinforcement of Polymer Nano-Composites*; Cambridge University Press: Cambridge, U.K., and New York, 2009.
(64) Cashell, E. M.; Douglas, D. C.; McBrierty, V. J. *Polymer J* **1978**, *10*, 557.
(65) Leu, G.; Liu, Y.; Werstler, D. D.; Cory, D. G. *Macromolecules* **2004**, *37*, 6883.
(66) O'Brien, J.; Cashell, E.; Wardell, G. E.; McBrierty, V. J. *Macromolecules* **1976**, *9*, 653.
(67) Cashell, E.; McBrierty, V. J. *J. Mater. Sci.* **1977**, *12*, 2011.
(68) Kenny, J. C.; McBrierty, V. J.; Rigbi, Z.; Douglas, D. C. *Macromolecules* **1991**, *24*, 436.
(69) Saalwächter, K.; Klüppel, M.; Luo, H.; Schneider, H. *Appl. Magn. Reson.* **2004**, *27*, 401.
(70) Bansal, A.; Yang, H.; Li, C.; Cho, K.; Benicewicz, B. C.; Kumar, S. K.; Schadler, L. S. *Nat. Mater.* **2005**, *4*, 693.
(71) Graf, R.; Demco, D. E.; Hafner, S.; Spiess, H. W. *Solid State Nucl. Magn. Reson.* **1998**, *12*, 139.
(72) Fechete, R.; Demco, D. E.; Blümich, B. *J. Magn. Reson.* **2004**, *169*, 19.
(73) Bertmer, M.; Demco, D. E.; Wang, M.; Melian, C.; Marcean-Celcea, R. I.; Fechete, R.; Baias, M.; Blümich, B. *Chem. Phys. Lett.* **2006**, *431*, 404.

(74) Orza, R. A.; Magusin, P. C. M. M.; Litvinov, V. M.; Duin van, M.; Michels, M. A. J. *Macromolecules* **2007**, *40*, 8999.
(75) Wu., G.; Asai, S.; Sumita, M.; Yui, H. *Macromolecules* **2002**, *35*, 945.
(76) Schröder, A.; Klüppel, M.; Schuster, R. H.; Heidberg, J. *Carbon* **2002**, *40*, 207.
(77) Schröder, A.; Klüppel, M.; Schuster, R. H. *Macromol. Mater. Eng.* **2007**, *292*, 885.
(78) Barendswaard, W.; Litvinov, V. M.; Souren, F.; Scherrenberg, R. L.; Gondard, C.; Colemonts, C. *Macromolecules* **1999**, *32*, 167.
(79) Gruber, T.; Zerda, T. W.; Gerspacher, M. *Carbon* **1994**, *32*, 1377.
(80) Hjelm, R.; Wampler, W. A.; Seeger, P. A.; Gerspacher, M. *J. Mater. Res.* **1994**, *9*, 3210.
(81) Xu, W.; Zerda, T. W.; Raab, H.; Goritz, D. *Carbon* **1997**, *35*, 471.
(82) Jones, R. A. L. *Curr. Opin. Colloid Interface Sci.* **2004**, *4*, 153.
(83) Morozov, I.; Lauke, B.; Heinrich, G. *Comput. Mater. Sci.* **2010**, *47*, 817.
(84) Dikland, H.; van Duin, M. In *Spectroscopy of Rubbery Materials*; Litvinov, V. M., De, P. P., Eds.; RAPRA Technology: Shawbury, U.K., 2002; p 207.
(85) Dupres, S.; Lomg, D. R.; Albouy, P.-A.; Sotta, P. *Macromolecules* **2009**, *42*, 2634.